An Optimized U-Net and MobileNetV2 Framework for Accurate and Efficient Brain Tumour Classification from MRI Images

R Elavarasi[1], S Murugesan[2*], S Ramalingam[3], P Kanimozhi[4], Harprith Kaur R S[5]

[1]*AMET Deemed to be University, Kanathur, Chennai 603112, India.*

[2]*St.Joseph University in Tanzania, Dar es salaam, 11007, Tanzania.*

[3]*Sri Eshwar College of Engineering, Kinathukadavu, Coimbatore 641202, India.*

[4]*Saranathan College of Engineering, Panjappur, Trichy 620012, India.*

[5]*Faculty of Data Science and IT, INTI International University, 71800 Nilai, Malaysia.*

(Received: January 25, 2026; Revised: March 25, 2026; Accepted: July 1, 2026; Available online: August 18, 2026)

Abstract

Accurate brain tumour identification from magnetic resonance imaging (MRI) requires models that can effectively localize tumour regions while maintaining high classification performance and computational efficiency. This study presents an integrated U-Net–MobileNetV2 framework for automated brain tumour analysis using MRI images. The proposed pipeline incorporates image thresholding, morphological processing, contour-based cropping, bicubic resizing, normalization, and data augmentation prior to model training. U-Net is employed to segment tumour regions and preserve diagnostically relevant spatial information, while MobileNetV2 performs lightweight classification using segmentation-guided representations. The dataset consists of 512 × 512-pixel brain MRI images divided into 80% training, 10% validation, and 10% testing subsets. Model performance is evaluated using accuracy, precision, recall, and F1-score and compared with CNN, Random Forest, Naïve Bayes, and Support Vector Machine classifiers. The proposed framework achieves 99.52% accuracy, 97.57% precision, 98.05% recall, and 97.81% F1-score, outperforming all evaluated baseline models. Compared with the strongest baseline, SVM, the proposed method improves accuracy by 1.43 percentage points. These results demonstrate that combining segmentation-driven tumour localization with lightweight deep feature learning provides an effective framework for accurate and computationally efficient MRI-based brain tumour classification.

Keywords: Brain Tumour Classification, Magnetic Resonance Imaging, U-Net, MobileNetV2, Deep Learning, Medical Image Segmentation, Process Innovation

1. Introduction

Brain tumours are among the most critical neurological abnormalities because their progression can substantially affect neurological function, treatment complexity, and patient survival. Magnetic Resonance Imaging (MRI) has become a primary imaging modality for brain-tumour assessment because it provides detailed soft-tissue contrast without ionizing radiation. However, the increasing volume and dimensionality of MRI data make manual interpretation and tumour delineation labor-intensive, observer-dependent, and susceptible to variability. Consequently, automated image-processing approaches have been extensively investigated to support tumour localization, segmentation, and diagnostic decision-making [1], [2]. Accurate segmentation is particularly important because subsequent measurements and classification decisions depend directly on the reliable identification of tumour regions.

Computational approaches for brain-tumour analysis have evolved from conventional image-processing pipelines toward machine-learning and deep-learning models. Earlier systems commonly relied on handcrafted descriptors derived from intensity, texture, morphology, edges, and statistical characteristics, followed by classifiers such as neural networks or other machine-learning algorithms [3], [4], [5]. Although these techniques demonstrated the feasibility of automated tumour recognition, their performance is strongly influenced by feature-engineering strategies and image quality. Statistical and machine-learning methods have subsequently improved tumour detection through more

***Corresponding author: S Murugesan (murugesanmepe@gmail.com)**
DOI: https://doi.org/10.47738/jads.v7i3.1468

systematic feature extraction and classification [6], while MRI-based frameworks combining lesion segmentation and discriminative features have achieved increasingly competitive diagnostic performance [7]. The introduction of convolutional neural networks (CNNs) further transformed brain MRI analysis by allowing hierarchical image representations to be learned directly from training data. CNN-based approaches have demonstrated strong performance in recognizing complex tumour characteristics without requiring extensive handcrafted feature design [8]. Nevertheless, segmentation remains a critical stage because irrelevant anatomical structures and background information can introduce unnecessary variability into classification models. Conventional approaches based on edge detection and intensity adjustment have therefore been investigated for isolating suspicious regions [9], [10], but their dependence on image-specific thresholds and predefined processing rules can reduce robustness across heterogeneous MRI samples.

Recent deep architectures have substantially improved brain-tumour analysis by learning increasingly discriminative representations from medical images. Deep CNN architectures have reported high classification performance for binary and multiclass brain-tumour recognition [11], while alternative learning schemes have explored combinations of texture descriptors and extreme-learning models for tumour identification [12]. More recent deep-learning-based MRI systems have also demonstrated highly accurate detection of glioma, meningioma, and pituitary tumours [13]. Despite these advances, high predictive performance alone does not fully address deployment requirements. Large networks may introduce considerable parameter counts, memory consumption, and inference costs, which can restrict their applicability in resource-constrained or real-time diagnostic environments.

This study addresses this limitation through an integrated segmentation–classification framework combining U-Net and MobileNetV2. U-Net is employed to identify and delineate tumour-related regions from MRI images so that subsequent analysis is concentrated on spatially relevant information rather than the complete image. The segmented representation is then processed using MobileNetV2, whose depthwise separable convolutions and inverted residual structures provide a comparatively lightweight classification architecture. The resulting pipeline therefore separates two complementary analytical objectives: spatial localization through U-Net and computationally efficient discriminative learning through MobileNetV2. Image preprocessing, normalization, augmentation, transfer learning, and hyperparameter optimization are incorporated to improve robustness and generalization across MRI samples.

The primary contribution of this work is a unified framework that combines tumour-region extraction and lightweight classification within a single analytical pipeline. Rather than applying classification directly to unstructured MRI images, the proposed method exploits segmentation-derived spatial information before predictive modeling, reducing the influence of irrelevant image regions and strengthening feature representation. The framework is evaluated using brain MRI data partitioned into training, validation, and testing subsets, and its predictive capability is quantified using accuracy, precision, and recall. This design provides a systematic basis for assessing whether accurate tumour recognition can be achieved while maintaining computational efficiency suitable for practical diagnostic-support applications.

2. Literature Review

Automated brain-tumour analysis has progressively shifted from handcrafted image-processing pipelines to representation-learning approaches. Earlier studies combined MRI preprocessing with neural networks, texture descriptors, statistical features, and conventional classifiers to distinguish tumour and non-tumour regions [14], [16], [17]. Large-scale image analysis subsequently demonstrated that deep convolutional representations could extract discriminative information directly from brain MRI data with less dependence on manually engineered features [18]. Related machine-learning systems also explored feature-based detection and computer-aided segmentation as mechanisms for reducing diagnostic variability [19], [20]. These developments are consistent with previous findings showing that CNN-based models can achieve high tumour-recognition performance [3], [7], [11], although performance remains sensitive to preprocessing, region localization, and the characteristics of the underlying dataset.

Recent research has increasingly treated segmentation as a critical analytical stage rather than merely an image-preprocessing operation. U-Net introduced an encoder–decoder architecture in which a contracting path captures contextual information while the expanding path reconstructs spatial detail for precise localization [21]. This design is

 ISSN 2723-6471

particularly suitable for medical images because tumour classification may depend not only on global appearance but also on localized morphological patterns. Benchmark datasets such as BraTS have further standardized evaluation by providing multimodal MRI scans with expert-annotated tumour regions, enabling systematic comparison of segmentation algorithms [23]. Recent lightweight U-Net variants have additionally attempted to preserve segmentation capability while reducing computational complexity and emphasizing diagnostically relevant tumour regions [24]. These advances extend earlier segmentation-oriented approaches based on edge and intensity information [9], [10] by enabling hierarchical spatial representations to be learned directly from data.

In parallel, efficient convolutional architectures have become increasingly important for tumour classification. MobileNetV2 introduced inverted residual blocks, linear bottlenecks, and depthwise convolutions to reduce computational operations and parameter requirements while retaining discriminative representation capacity [22]. Such characteristics provide an alternative to deeper and computationally heavier CNN architectures previously applied to brain-tumour recognition [11], [13]. Studies combining segmentation and classification have also shown that separating tumour localization from subsequent multiclass prediction can provide a structured learning pipeline in which the classifier operates on more informative image regions [15], [25]. This approach is particularly relevant when MRI datasets contain substantial background anatomy that may otherwise contribute redundant information during model training.

Despite these developments, existing studies frequently emphasize either segmentation accuracy or classification performance independently, while comparatively less attention is given to integrating spatial localization, predictive discrimination, and computational efficiency within a unified workflow. U-Net provides a strong mechanism for preserving tumour morphology and boundary information [21], whereas MobileNetV2 offers an efficient feature-learning architecture suitable for lower-complexity inference [22]. The combination therefore provides a complementary segmentation–classification strategy in which tumour-specific representations can be generated before predictive modeling. Building on the high classification performance reported in recent brain-tumour studies [11], [13], [15] and the development of efficient segmentation architectures [23], [24], the present study investigates whether an integrated U-Net–MobileNetV2 pipeline can simultaneously maintain strong predictive performance and a computationally efficient model structure.

3. Methodology

3.1. Dataset and Image Preprocessing

The experimental pipeline was developed using the brain MRI dataset described in the original study, consisting of images with a spatial resolution of 512 × 512 pixels and tumour annotations used for model development. The dataset was partitioned into 80% training data, 10% validation data, and 10% testing data. The training subset was used to estimate model parameters, the validation subset was used to monitor generalization during model development, and the independent test subset was retained for final performance evaluation. This separation prevents test observations from influencing parameter estimation and provides a consistent basis for comparing the proposed framework with conventional classifiers. Automated MRI analysis is particularly dependent on reliable preprocessing because variations in background anatomy, image boundaries, and irrelevant regions can affect the discriminative representations learned by neural networks [3].

Each MRI image was processed using a sequential preprocessing pipeline consisting of thresholding, morphological refinement, contour localization, extreme-point cropping, resizing, normalization, and data augmentation. Thresholding was initially applied to obtain a binary representation of the brain region. Morphological dilation and erosion were subsequently used to reduce isolated artifacts and refine the detected structure. The largest contour was identified, followed by computation of four extreme coordinates representing the topmost, bottommost, leftmost, and rightmost points. These coordinates defined the crop boundary used to remove non-informative background regions. The cropped images were subsequently resized using bicubic interpolation, which preserves smoother intensity transitions during spatial resampling. For an input image (I), intensity normalization can be expressed as

 ISSN 2723-6471

$$\frac{I(x,y) - I_{min}}{I_{max} - I_{min}}, \tag{1}$$

I(x,y) denotes the original pixel intensity, while I_{min}d I_{max} present the minimum and maximum intensity values within the image. The transformation maps image intensities into a consistent numerical range before model optimization. Data augmentation was subsequently applied to the training data to increase image variability and reduce overfitting.

Figure 1 illustrates the end-to-end workflow of the proposed MRI-based brain tumour classification framework, beginning with the input MRI dataset and ending with the predicted tumour class. First, the MRI images undergo preprocessing, including thresholding to obtain a binary brain mask, morphological refinement, cropping of the region of interest, resizing, and intensity normalization to reduce irrelevant background information and ensure consistent input dimensions. The preprocessed images are then processed by a U-Net segmentation model to localize the tumour region and generate a segmented representation of the lesion. The resulting tumour region is subsequently used as the input representation for the MobileNetV2 classifier, which acts as a lightweight feature extractor followed by a softmax classification layer. Finally, the framework assigns each MRI image to one of four classes: Glioma, Meningioma, Pituitary, or No Tumour. Thus, as shown in figure 1, the complete pipeline integrates image preprocessing, tumour localization, and lightweight deep-learning classification into a sequential framework designed for automated brain tumour diagnosis.

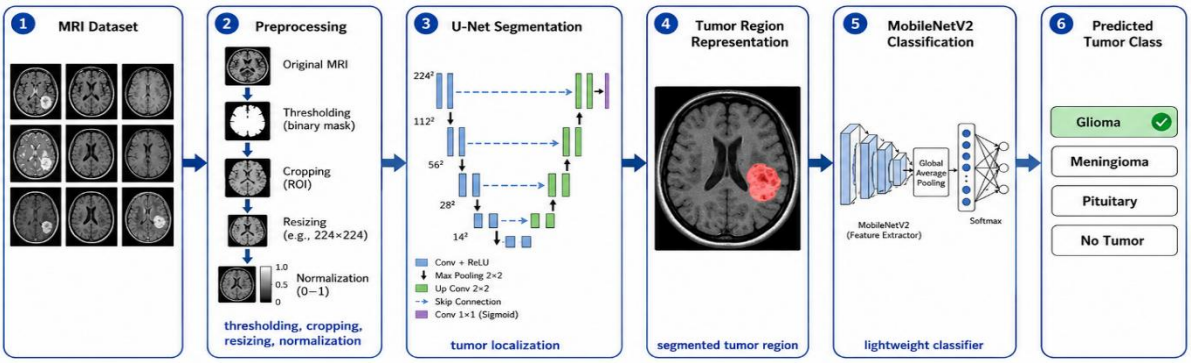

Figure 1. End-to-end MRI preprocessing, segmentation, and classification workflow

3.2. 3U-Net–MobileNetV2 Segmentation and Classification Framework

The proposed framework follows a two-stage learning strategy in which tumour localization and tumour classification are treated as interconnected but distinct computational tasks. In the first stage, U-Net receives the preprocessed MRI image and produces a spatial representation of the tumour region. Its encoder progressively transforms the input into increasingly abstract feature maps, whereas the decoder reconstructs spatial information through upsampling and skip connections. These skip connections allow high-resolution information from the encoder to be combined with deeper semantic representations, thereby retaining tumour-boundary information required for subsequent analysis [21]. Let the segmentation network be represented by

$$\widehat{M} = f_{\theta}(X), \tag{2}$$

(X) denotes the preprocessed MRI image, f_{θ} represents the U-Net parameterized by θ, and $\widehat{M}$ denotes the predicted tumour-region representation. The segmented representation is subsequently used to emphasize tumour-specific spatial information before classification. The extracted region contains characteristics associated with tumour morphology, including spatial distribution, shape, intensity variation, and texture-related information [25], [26].

In the second stage, the segmentation-derived representation is processed by MobileNetV2. MobileNetV2 was selected because its inverted residual blocks and depthwise separable convolutions substantially reduce computational requirements compared with conventional convolutional operations while preserving hierarchical representation capability [22]. For an input feature tensor, depthwise separable convolution decomposes conventional convolution into depthwise and pointwise operations. Its approximate computational cost can be expressed as

$$D_K^2 D_F^2 M + D_F^2 MN, \tag{3}$$

D_K is the kernel dimension, D_F is the spatial dimension of the feature map, (M) is the number of input channels, and (N) is the number of output channels. In comparison, a standard convolution requires

$$D_K^2 D_F^2 MN. \tag{4}$$

This decomposition reduces redundant computation and supports a lightweight classification stage. The final class probabilities are generated using the Softmax function,

$$e^{z_k} \sum_{j=1}^{K} e^{z_j}, \tag{5}$$

z_k represents the output score associated with class (k), and (K) denotes the total number of target classes. The predicted class is obtained as

$$\arg\max_k P\,(y = k|z) \tag{6}$$

Transfer learning was used to initialize the MobileNetV2 representation, followed by task-specific model adaptation using the MRI training samples. In this configuration, U-Net provides localized spatial information while MobileNetV2 performs discriminative representation learning and final classification. Following the initial preprocessing described in figure 1, the detailed preprocessing operations applied to a representative MRI image are presented in figure 2. The figure shows the transformation from the original MRI image through thresholding and morphological processing to isolate the brain region, followed by largest-contour detection and extreme-point cropping to remove irrelevant background areas. The resulting region of interest is then resized to (512 x 512) pixels and normalized to the range of 0–1. These sequential operations provide a standardized MRI representation while reducing irrelevant background information and preserving the anatomical region required for subsequent tumour segmentation and classification.

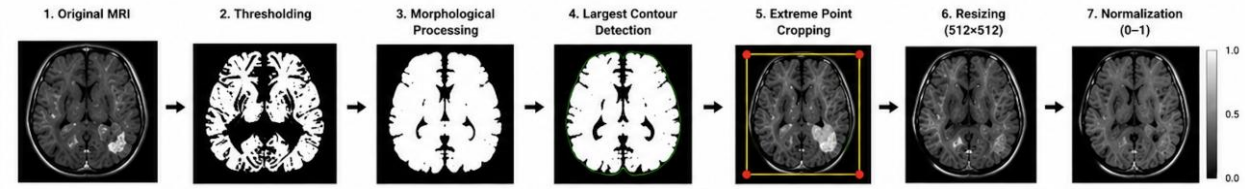

Figure 2. Representative MRI preprocessing and tumour-region extraction

The tumour localization process using the U-Net architecture is illustrated in figure 3. The preprocessed MRI image is first passed through the U-Net encoding path, where successive downsampling operations extract increasingly high-level spatial representations while reducing the feature-map dimensions. The bottleneck provides a compact representation of the input, after which the decoding path progressively restores the spatial resolution through upsampling. Skip connections transfer spatial information from the corresponding encoder layers to the decoder, helping preserve fine-grained tumour boundaries. The resulting segmentation output is converted into a tumour mask, which is overlaid on the original MRI to visualize the localized lesion. Finally, the segmented tumour region is extracted as the spatially focused representation used for subsequent MobileNetV2-based classification. Transfer learning is then applied to initialize the MobileNetV2 feature extractor, followed by task-specific adaptation using the MRI training samples. In this configuration, U-Net provides localized tumour-region information, whereas MobileNetV2 learns discriminative visual representations from the extracted region and performs the final tumour-class prediction.

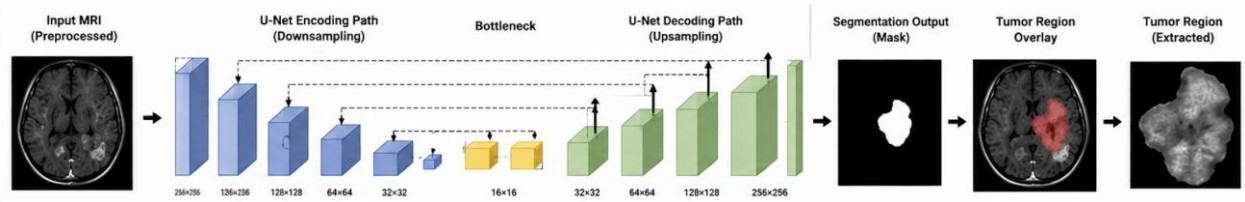

Figure 3. Representative U-Net tumour feature extraction results

ISSN 2723-6471

4. Results and Discussion

4.1. Extracted Tumour Feature Characteristics

The segmentation results obtained using the U-Net model are illustrated in figure 4. The figure presents four representative MRI samples, with the original MRI images shown in the left column, the predicted tumour masks in the center column, and the resulting segmented or masked MRI images in the right column. The predicted masks identify the spatial location of the tumour regions, while the overlay visualization demonstrates how the detected regions correspond to the abnormal areas in the original MRI images. Across the representative samples, the U-Net model successfully localizes tumours with different sizes, shapes, and spatial positions, providing a focused representation of the lesion for subsequent feature extraction and classification.

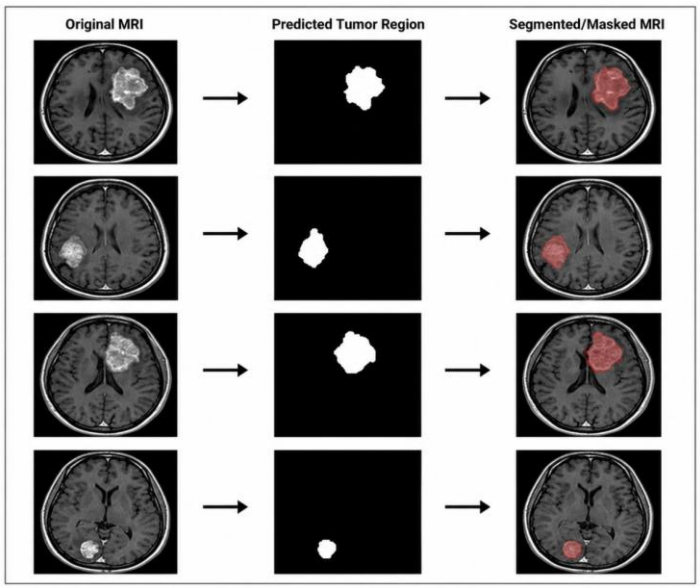

Figure 4. Representative U-Net segmentation results

Following tumour segmentation, quantitative features were extracted from the detected MRI regions to characterize their local intensity variation and structural properties. The extracted features consisted of contrast, dissimilarity, homogeneity, and energy. Contrast and dissimilarity describe the degree of local intensity variation within the segmented region, whereas homogeneity and energy characterize the uniformity and distribution of intensity patterns. The extracted values for six representative MRI samples are presented in table 1.

Table 1. Extracted features from segmented MRI regions

Image	Contrast	Dissimilarity	Homogeneity	Energy
1	282.34	2.03	0.98	0.97
2	98.04	0.61	0.97	0.90
3	341.26	1.72	0.96	0.93
4	359.36	2.46	0.98	0.96
5	150.04	0.35	0.95	0.98
6	361.05	1.42	0.98	0.95

As shown in table 1, the extracted features exhibit different levels of variation across the representative MRI regions. Contrast ranges from 98.04 to 361.05, while dissimilarity ranges from 0.35 to 2.46, indicating considerable differences in local intensity transitions among the segmented regions. In contrast, homogeneity remains within a relatively narrow range of 0.95–0.98, and energy ranges from 0.90 to 0.98. These complementary characteristics provide information

about both intensity variation and local structural organization within the detected tumour regions. The descriptive statistics calculated from the six representative samples are summarized in table 2.

Table 2. Descriptive statistics of extracted MRI features

Feature	Mean	SD	Minimum	Maximum
Contrast	265.35	114.31	98.04	361.05
Dissimilarity	1.43	0.82	0.35	2.46
Homogeneity	0.970	0.013	0.95	0.98
Energy	0.948	0.029	0.90	0.98

As shown in table 2, contrast and dissimilarity exhibit substantially greater variation than homogeneity and energy. The relatively large standard deviation of contrast (114.31) indicates considerable differences in intensity variation among the evaluated regions, while dissimilarity also shows noticeable variability with a standard deviation of 0.82. Conversely, homogeneity and energy remain relatively stable, with standard deviations of 0.013 and 0.029, respectively. This suggests that the extracted feature set provides complementary information, combining features that capture intensity variation with features that describe the consistency of local texture patterns.

It should be noted that the statistics in Table 3 are calculated from the six representative samples shown in Table 2 and therefore should not be interpreted as population-level statistics for the entire MRI dataset. If these features were extracted from the complete dataset, the manuscript should report the statistics calculated across all available segmented regions to provide a more representative quantitative analysis.

4.2. Classification Performance

The proposed U-Net–MobileNetV2 framework was evaluated against four baseline approaches, namely Convolutional Neural Network (CNN), Random Forest (RF), Naïve Bayes (NB), and Support Vector Machine (SVM). The classification performance of all evaluated methods was assessed using accuracy, precision, recall, and F1-score. The comparative results are presented in table 3.

Table 3. Performance comparison of the evaluated models

Method	Accuracy (%)	Precision (%)	Recall (%)	F1-score (%)
CNN	95.27	94.71	95.06	94.88
RF	96.58	95.26	96.48	95.87
NB	97.36	95.99	97.19	96.59
SVM	98.09	96.38	97.73	97.05
U-Net–MobileNetV2	99.52	97.57	98.05	97.81

As shown in table 3, the proposed U-Net–MobileNetV2 framework achieved the highest performance across all four evaluation metrics, with an accuracy of 99.52%, precision of 97.57%, recall of 98.05%, and F1-score of 97.81%. Among the baseline methods, SVM achieved the strongest performance, with an accuracy of 98.09% and an F1-score of 97.05%. RF and NB achieved lower but still competitive performance, whereas the conventional CNN produced the lowest accuracy and F1-score among the evaluated approaches. For a more direct comparison, the performance differences between the proposed framework and the strongest baseline, SVM, are quantified as follows. The proposed method improved accuracy by 1.43 percentage points, precision by 1.19 percentage points, recall by 0.32 percentage points, and F1-score by 0.76 percentage points. These results suggest that incorporating tumour-region localization through U-Net before MobileNetV2 classification can provide more discriminative representations than using the baseline classifiers alone. The comparison between the proposed framework and the conventional CNN is further illustrated in figure 5.

ISSN 2723-6471

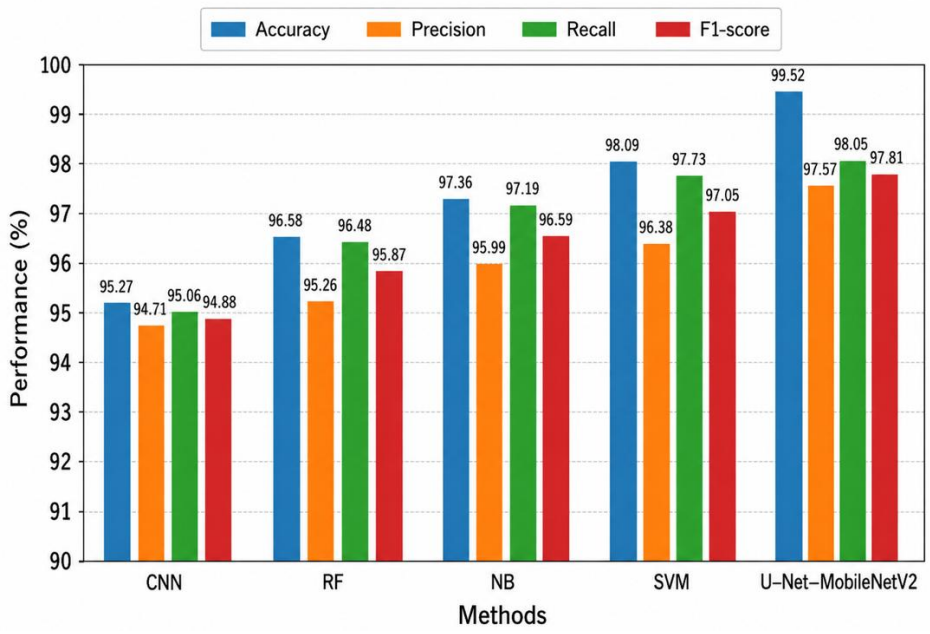

Figure 5. Classification performance comparison

As shown in figure 5, the U-Net–MobileNetV2 framework consistently achieves higher values across accuracy, precision, recall, and F1-score than the four baseline methods. Compared with CNN, the proposed framework increases accuracy from 95.27% to 99.52%, corresponding to an absolute improvement of 4.25 percentage points. Precision increases by 2.86 percentage points, while recall improves by 2.99 percentage points. The F1-score also increases from 94.88% to 97.81%, representing an improvement of 2.93 percentage points.

The improvement over the baseline models suggests that the two-stage design contributes to classification performance by separating tumour localization from discriminative classification. U-Net focuses the input representation on the relevant tumour region, while MobileNetV2 provides lightweight feature extraction and classification. Nevertheless, these results should be interpreted as a comparison under the specific experimental configuration and dataset used in this study. A fair comparison requires that all baseline models use the same training, validation, and testing partitions and, where applicable, comparable preprocessing and evaluation procedures.

4.3. Comparative Analysis

A progressive improvement in predictive performance is observed across the evaluated models. CNN recorded the lowest accuracy at 95.27%, followed by RF at 96.58%, NB at 97.36%, and SVM at 98.09%. The proposed U-Net–MobileNetV2 framework further increased accuracy to 99.52%. A similar pattern is observed for precision and recall, indicating that the improvement is not limited to overall classification accuracy but is also reflected in the model's ability to reduce incorrect positive predictions and correctly identify relevant tumor observations.

The result can be attributed to the separation of spatial localization and class discrimination within the proposed pipeline. Rather than requiring the classifier to learn simultaneously from tumor regions and irrelevant anatomical background, U-Net first constrains the representation toward diagnostically relevant regions. MobileNetV2 subsequently performs classification using this localized representation while benefiting from its inverted residual and depthwise separable convolution architecture [21], [22]. This structure provides a direct connection between segmentation quality and downstream predictive performance.

The obtained accuracy of 99.52% is also consistent with the high predictive performance reported by recent deep-learning-based brain-tumour studies [11], [13], while providing an architecture explicitly structured around segmentation followed by lightweight classification. Overall, the experimental results demonstrate that incorporating tumour-region localization before classification produces the strongest performance among the evaluated methods, with the largest improvement observed in accuracy and consistently higher precision, recall, and F1-score.

4.4. Discussion

The experimental results demonstrate that the proposed U-Net–MobileNetV2 framework provides strong performance for brain tumour classification from MRI images. The model achieved an accuracy of 99.52%, precision of 97.57%, recall of 98.05%, and F1-score of 97.81%, outperforming CNN, Random Forest, Naïve Bayes, and SVM. This result indicates that integrating tumour-region segmentation with lightweight deep feature extraction can provide a more discriminative representation than applying classification directly to the MRI images.

The performance improvement can be attributed primarily to the segmentation stage. U-Net is designed to preserve both contextual and spatial information through its encoder–decoder structure and skip connections, making it particularly suitable for identifying irregular tumour boundaries [21]. Previous research has also demonstrated that U-Net-based segmentation can provide useful tumour-region representations for subsequent classification tasks [23], [24]. In this study, the segmented tumour regions allow MobileNetV2 to focus on diagnostically relevant areas while reducing the influence of surrounding anatomical structures and background information. A similar segmentation-before-classification strategy has been reported to improve automated brain tumour prediction by providing the classifier with a more focused representation of the MRI image [25].

The results are also consistent with earlier studies demonstrating the effectiveness of deep learning for brain tumour detection and classification. Deep CNN-based approaches have achieved strong performance by automatically learning hierarchical representations from MRI images, reducing dependence on manually designed features [3], [11]. Similarly, advanced deep-learning approaches have demonstrated high performance for multiclass brain tumour recognition [13], [15]. The present study extends these findings by combining segmentation and classification rather than treating the two tasks independently.

The proposed model achieved a 1.43 percentage-point improvement in accuracy over SVM, which was the strongest conventional baseline in this study. This improvement suggests that automatically learned deep representations can capture more complex spatial and visual characteristics than conventional machine-learning classifiers. Previous studies using statistical and machine-learning methods have shown that algorithms such as SVM and other classifiers can perform effectively when informative features are available [5], [6], [12]. However, their performance is generally dependent on the quality of the extracted features. In contrast, the proposed framework allows U-Net and MobileNetV2 to learn task-relevant representations directly from the MRI data.

Another important aspect of the proposed framework is the use of MobileNetV2 as the classification backbone. MobileNetV2 employs inverted residual blocks and depthwise separable convolutions to reduce computational complexity while maintaining effective feature extraction [22]. This makes it attractive for medical-image applications in which computational efficiency is important. Previous research has also explored MobileNetV2 as an encoder or feature extractor for brain tumour analysis and reported that lightweight architectures can maintain strong performance while reducing computational requirements [22], [24]. Therefore, the combination of U-Net and MobileNetV2 provides complementary capabilities: U-Net emphasizes spatial localization, while MobileNetV2 provides efficient discriminative feature learning.

The extracted texture characteristics provide additional evidence that the segmented tumour regions contain meaningful visual information. Contrast and dissimilarity exhibited greater variation across the representative MRI samples, whereas homogeneity and energy were relatively stable. These characteristics are consistent with the importance of intensity and texture information in conventional brain tumour analysis [1], [6]. However, rather than depending exclusively on handcrafted texture descriptors, the proposed framework uses the segmented image as input to a deep feature extractor. Consequently, the model can potentially learn more complex spatial relationships that cannot be fully represented by a small set of manually selected texture features.

The accuracy of 99.52% obtained in this study is comparable to the high performance reported by recent integrated segmentation–classification frameworks. For example, studies combining U-Net with deep classification networks have reported strong classification performance, supporting the idea that tumour localization can enhance subsequent classification [15], [25]. More recent research has similarly demonstrated that integrating segmentation and classification can achieve very high predictive performance while providing additional information about tumour

location [24]. These findings strengthen the argument that segmentation-guided classification is a promising direction for automated brain tumour analysis.

Nevertheless, the reported performance should be interpreted within the context of the dataset and experimental configuration used in this study. Differences in datasets, class distributions, preprocessing procedures, image acquisition protocols, and evaluation strategies can substantially affect reported accuracy. Therefore, the 99.52% accuracy should not be interpreted as evidence that the proposed framework universally outperforms every previously published brain tumour model. Instead, the result demonstrates that, under the same experimental conditions, the proposed U-Net–MobileNetV2 architecture provides better performance than the baseline models evaluated in this study.

A further consideration is that the segmentation quality itself was not quantitatively evaluated using segmentation-specific metrics such as Dice coefficient or intersection over union. This limits the ability to determine the direct relationship between segmentation accuracy and classification performance. Previous studies have emphasized the importance of quantitative segmentation evaluation when developing automated brain tumour systems [23], [24]. Future experiments should therefore evaluate both stages independently, allowing the effect of segmentation quality on final classification performance to be examined more rigorously.

Overall, the findings indicate that the integration of U-Net and MobileNetV2 is effective because the two architectures address complementary aspects of MRI analysis. U-Net provides spatially focused tumour localization [21], while MobileNetV2 provides efficient deep feature extraction [22]. The resulting 99.52% classification accuracy, together with the improvements in precision, recall, and F1-score over the evaluated baselines, suggests that segmentation-guided lightweight classification is a promising approach for automated brain tumour analysis.

5. Conclusion

This study developed an integrated U-Net–MobileNetV2 framework for automated brain-tumor analysis from MRI images. The proposed pipeline combines preprocessing, tumor-region segmentation, feature representation, and lightweight classification within a structured workflow. U-Net was used to localize diagnostically relevant tumor regions, while MobileNetV2 performed final classification using segmentation-guided representations.

The experimental results showed that the proposed framework achieved 99.52% accuracy, 97.57% precision, 98.05% recall, and 97.81% F1-score, outperforming CNN, Random Forest, Naïve Bayes, and SVM. Compared with the strongest baseline, SVM, the proposed model improved accuracy by 1.43 percentage points and F1-score by approximately 0.76 percentage points. The extracted MRI features also showed meaningful variation in contrast and dissimilarity while maintaining consistently high homogeneity and energy values, supporting the effectiveness of the segmentation stage in preserving relevant structural information.

Overall, the results indicate that separating tumour localization from classification can improve predictive performance while maintaining a computationally efficient architecture. The combination of U-Net and MobileNetV2 therefore provides a promising approach for accurate MRI-based brain-tumour classification, particularly for applications requiring both high predictive performance and relatively lightweight inference. Future work can extend the framework through larger multi-center MRI datasets, multimodal imaging, attention-based segmentation, and external validation to further evaluate its generalizability and clinical robustness.

6. Declarations

6.1. Author Contributions

Conceptualization: R.E., S.M.; Methodology: R.E., S.R.; Software: P.K., H.K.R.S.; Validation: S.M., S.R.; Formal Analysis: R.E.; Investigation: P.K., H.K.R.S.; Resources: S.M., S.R.; Data Curation: R.S.; Writing – Original Draft Preparation: R.E.; Writing – Review and Editing: S.M., H.K.R.S.; Visualization: P.K.; All authors have read and agreed to the published version of the manuscript.

6.2. Data Availability Statement

The data presented in this study are available on request from the corresponding author.

6.3. Funding

The authors received no financial support for the research, authorship, and/or publication of this article.

6.4. Institutional Review Board Statement

Not applicable.

6.5. Informed Consent Statement

Not applicable.

6.6. Declaration of Competing Interest

The authors declare that they have no known competing financial interests or personal relationships that could have appeared to influence the work reported in this paper.

References

[1] V. Y. Borole, S. S. Nimbhore, and D. S. S. Kawthekar, "Image processing techniques for brain tumour detection: A review," *Int. J. Emerg. Trends Technol. Comput. Sci.*, vol. 4, no. 5, pp. 1–10, Sep. 2015.

[2] S. Roy, S. Nag, I. K. Maitra, and S. K. Bandyopadhyay, "A review on automated brain tumour detection and segmentation from MRI of brain," *arXiv*, vol. 2013, no. Dec., pp. 1–12, Dec. 2013.

[3] M. Nazir, S. Shakil, and K. Khurshid, "Role of deep learning in brain tumour detection and classification (2015 to 2020): A review," *Comput. Med. Imaging Graph.*, vol. 91, no. Aug., pp. 1–12, Aug. 2021, doi: 10.1016/j.compmedimag.2021.101940.

[4] P. Sapra, R. Singh, and S. Khurana, "Brain tumour detection using neural network," *Int. J. Sci. Modern Eng.*, vol. 2013, no. Jan., pp. 1–6, Jan. 2013.

[5] K. Sharma, A. Kaur, and S. Gujral, "Brain tumour detection based on machine learning algorithms," *Int. J. Comput. Appl.*, vol. 103, no. 1, pp. 1–5, Oct. 2014.

[6] J. Amin, M. Sharif, M. Raza, T. Saba, and M. A. Anjum, "Brain tumour detection using statistical and machine learning method," *Comput. Methods Programs Biomed.*, vol. 177, no. Aug., pp. 69–79, Aug. 2019.

[7] J. Amin, M. Sharif, M. Yasmin, and S. L. Fernandes, "A distinctive approach in brain tumour detection and classification using MRI," *Pattern Recognit. Lett.*, vol. 139, no. Nov., pp. 118–127, Nov. 2020.

[8] T. Hossain, F. S. Shishir, M. Ashraf, M. A. Al Nasim, and F. M. Shah, "Brain tumour detection using convolutional neural network," *ICASERT*, vol. 2019, no. Dec., pp. 1–6, Dec. 2019.

[9] P. Sharma, M. Diwakar, and S. Choudhary, "Application of edge detection for brain tumour detection," *Int. J. Comput. Appl.*, vol. 58, no. 16, pp. 1–6, Nov. 2012.

[10] P. G. Rajan and C. Sundar, "Brain tumour detection and segmentation by intensity adjustment," *J. Med. Syst.*, vol. 43, no. 8, pp. 1–10, Aug. 2019, doi: 10.1007/s10916-019-1389-5.

[11] M. S. I. Khan, A. Rahman, T. Debnath, M. R. Karim, M. K. Nasir, S. S. Band, *et al.*, "Accurate brain tumour detection using deep convolutional neural network," *Comput. Struct. Biotechnol. J.*, vol. 20, no. Oct., pp. 4733–4745, Oct. 2022.

[12] M. Sharif, J. Amin, M. Raza, M. A. Anjum, H. Afzal, and S. A. Shad, "Brain tumour detection based on extreme learning," *Neural Comput. Appl.*, vol. 32, no. Sep., pp. 15975–15987, Sep. 2020.

[13] A. B. Abdusalomov, M. Mukhiddinov, and T. K. Whangbo, "Brain tumour detection based on deep learning approaches and magnetic resonance imaging," *Cancers*, vol. 15, no. 16, pp. 1–15, Aug. 2023, doi: 10.3390/cancers15164172.

[14] M. Siar and M. Teshnehlab, "Brain tumour detection using deep neural network and machine learning algorithm," *ICCKE*, vol. 2019, no. Oct., pp. 363–368, Oct. 2019.

[15] T. Sadad, A. Rehman, A. Munir, T. Saba, U. Tariq, N. Ayesha, and R. Abbasi, "Brain tumour detection and multi-classification using advanced deep learning techniques," *Microsc. Res. Tech.*, vol. 84, no. 6, pp. 1296–1308, Jun. 2021.

[16] L. Kapoor and S. Thakur, "A survey on brain tumour detection using image processing techniques," *Confluence*, vol. 2017, no. Mar., pp. 582–585, Mar. 2017.

[17] H. E. M. Abdalla and M. Y. Esmail, "Brain tumour detection by using artificial neural network," *ICCCEEE*, vol. 2018, no. Nov., pp. 1–6, Nov. 2018.

[18] J. Amin, M. Sharif, M. Yasmin, and S. L. Fernandes, "Big data analysis for brain tumour detection: Deep convolutional neural networks," *Future Gener. Comput. Syst.*, vol. 87, no. Oct., pp. 290–297, Oct. 2018.

[19] G. Hemanth, M. Janardhan, and L. Sujihelen, "Design and implementing brain tumour detection using machine learning approach," *ICOEI*, vol. 2019, no. Apr., pp. 1289–1294, Apr. 2019.

[20] M. U. Akram and A. Usman, "Computer aided system for brain tumour detection and segmentation," *ICCNIT*, vol. 2011, no. Jul., pp. 299–302, Jul. 2011.

[21] O. Ronneberger, P. Fischer, and T. Brox, "U-Net: Convolutional networks for biomedical image segmentation," *MICCAI*, vol. 2015, no. Oct., pp. 234–241, Oct. 2015.

[22] M. Sandler, A. Howard, M. Zhu, A. Zhmoginov, and L.-C. Chen, "MobileNetV2: Inverted residuals and linear bottlenecks," *CVPR*, vol. 2018, no. Jun., pp. 4510–4520, Jun. 2018, doi: 10.1109/CVPR.2018.00474.

[23] B. H. Menze, A. Jakab, S. Bauer, J. Kalpathy-Cramer, K. Farahani, J. Kirby, *et al.*, "The multimodal brain tumour image segmentation benchmark (BRATS)," *IEEE Trans. Med. Imaging*, vol. 34, no. 10, pp. 1993–2024, Oct. 2015, doi: 10.1109/TMI.2014.2377694.

[24] K. Avazov, S. Mirzakhalilov, S. Umirzakova, A. Abdusalomov, and Y. I. Cho, "Dynamic focus on tumour boundaries: A lightweight U-Net for MRI brain tumour segmentation," *Bioengineering*, vol. 11, no. 12, pp. 1–15, Dec. 2024, doi: 10.3390/bioengineering11121302.

[25] B. Amin, R. S. Samir, Y. Tarek, M. Ahmed, R. Ibrahim, M. Ahmed, and M. Hassan, "Brain tumour multi classification and segmentation in MRI images using deep learning," *arXiv*, vol. 2023, no. Apr., pp. 1–15, Apr. 2023, doi: 10.48550/arXiv.2304.10039.

[26] S. Kumar, J. Singh, P. Singh, M. Diwakar, I. Gupta, V. Ravi, and S. S. Maidin, "Enhancing brain tumor segmentation using Berkeley wavelet transformation and improved SVM," *The Open Bioinformatics Journal*, vol. 18, no. 1, pp. 1-12, 2025.